Effects of 1D and 2D nanofillers in basalt/ Poly(Lactic Acid) composites for additive manufacturing

Aldobenedetto Zotti[1*], Simona Zuppolini[1], Tamás Tábi[2,3*], Marzio Grasso[4], Gougang Ren[4], Anna Borriello[1] and Mauro Zarrelli[1]

[1] Institute of Polymers, Composites and Biomaterials of National Research Council of Italy, 80055, Portici (NA), Italy

[2] MTA–BME Research Group for Composite Science and Technology, Muegyetem rkp. 3., H-1111 Budapest, Hungary

[3] Department of Polymer Engineering, Faculty of Mechanical Engineering, Budapest University of Technology and Economics, Muegyetem rkp. 3., H-1111 Budapest, Hungary

[4] School of Engineering and Technology, University of Hertfordshire, Hatfield AL10 9AB, UK

Abstract.

In this work, basalt microfiber reinforced poly(lactic acid) (PLA) composites filled with talc nanoplatelets (2D) and sepiolite nanofibers (1D) were prepared at different compositions and tested to assess the effects of filler geometry. Thermal analysis results show that crystallinity of amorphous PLA can be enhanced up to 24% by adding basalt and talc. Thermal stability of PLA is increased by basalt microfibers whereas talc and sepiolite prompted early degradation in binary composites. In ternary systems, i.e. PLA/basalt/talc and PLA/basalt/sepiolite, thermal stability was further increased. Mechanical tensile and flexural properties were remarkably increased for a specific composition basalt (30 wt%) and talc (10 wt%) with a final enhancement of 176% and 261% for modulus and 46% and 43% for strength respectively in tensile and bending configuration. For the composition, the coefficient of thermal expansion is significantly reduced up to 54% of the corresponding pristine PLA value. The increase of thermal conductivity is mainly related to the presence of 1D sepiolite, with a variation of ~54% for the 10 wt% PLA/sepiolite binary system. Finally, a significant increment of impact property was observed by unnotched Charpy impact tests for talc (+97%) and basalt (+140%) composites.

Keywords: A. Polymer-matrix composites (PMCs); B. Microstructures; C. Mechanical testing; C. Thermal analysis; Poly(Lactic Acid).

1. Introduction

Recently, because of the global waste management problems caused by short life cycle packaging applications, the research on renewable and biodegradable resources is becoming increasingly important. PLA, as one of the most promising biodegradable polymers, has the potential to replace engineering composites by reinforcements such as mineral ~~fibre~~fibers like basalt and sepiolite [1, 2]. PLA is an aliphatic,

thermoplastic, semi-crystalline polymer, with high strength (tensile strength ~65 MPa) and stiffness (elasticity modulus ~3 GPa).

PLA is among the thermopastic materials mainly used for 3D printing in different area such as medical and clinical applications, food packaging, toys and consumer 3D printing elements. As biopolymer it offers enviromental benefits including biodegradability, renewability and less gas emission which coul be driven the attention of such material also in advanced technology application for aerospace or automotive specifically requesting thermosetting polymers as epoxy or polyester for their inherently high specific properties. As the 3d printers have become more affordable and the industry technology is applying this process more complex geometry and different composnent, PLA is attactting the attention such as ideal material for many 3d printed parts or elements with the main advantage of being enviromental friendly, easy to process and characterised by a low coefficient of thermal expansion which significantly reduce effects of wraping to the printed surface and dimensional deformation for printed part.

Unfortunately, PLA is characterised by a low impact strength, i.e. ~25 kJ/m^2 by Charpy on an unnotched impact specimen; low deflection temperature under load and relatively poor thermal conductivity which does not facilitate the tempertaure uniformity of the fused flow of 3D printer nozzle during printing operations. Moreover, one of the PLA's significant drawbacks is its low crystallinity, which consequently influences its thermomechanical properties (tensile strenght, failure elongation and thermal degradation).

A research work employed numerous nucleating agents to overcome the problem of poor crystallization in the PLA, i.e. the uses of talc minerals [3, 4], microcrystalline cellulose [5], cellulose nanowhiskers [6], ethylene bis-stearamide (EBS) [7], silver nanoparticles [8] and carbon fiber [9].

Basalt ~~fibre~~fibers are commonly used as reinforcement in thermoplastic matrix composites [10-11]. It was proved that the natural volcanic rock based basalt ~~fibre~~fibers are excellent reinforcements for the PLA [12]. For examples using 30wt% of short basalt fibers, processed with PLA through conventional extrusion and injection moulding processes, it is possible to achieve a tensile strength of 120 MPa and a flexural strength of 180 MPa; moreover, tensile and flexural modulus are increased up to 7.6 GPa and 10.4 GPa, respectively, while the unnotched Charpy impact strength reaches the value of 38 kJ/m2 [11].

Talc is an excellent nucleating agent for PLA [13, 14] and may be used to develop high crystallinity during processing. Talc ($Mg_3Si_4O_{10}(OH)_2$) is a 2:1 tri-octahedral layered silicate having three octahedral Mg positions per four tetrahedral Si positions. This hydrated magnesium silicate is available in the form of sheets, which are simple to disperse in a polymer matrix because of the weak van der Walls interactions between platelets [15]. *Russo et al.* [16] have reported an increase in the crystallinity and the reduction in

the mean crystal size by the addition of poly(e-caprolactone) (PCL) which, together with talc nanoparticles, allow the formation of a large domain of PLA at the interface of immiscible PCL.

The presence of a second filler (talc) also enhances thermomechanical properties such as the HDT: it increases up to 175% confirming that the ternary system (PLA/PCL/talc) could be a more performing choice than the simple binary system (PLA/PCL). A PLA/talc composite was studied by Huda et al. [17] founding a significant improvement in flexural and tensile properties compared to that of neat PLA. Its tensile properties were higher than that of neat PLA because of stress transferability of the talc in PLA reinforced polymer composites [18].

Sepiolite has the structural formula of $Si_{12}Mg_8O_{30}(OH)_4(OH_2)_4 \cdot 8H_2O$, a typical magnesium silicate with the fibrous morphology with fine microporous channels close to 0.37 nm × 1.06 nm. The size of the ~~fibre~~fibers varies, from 10–5000 nm long, 10–30 nm wide, and 5–10 nm thick. The main feature is related to the presence of small channels across the fibrous structure of sepiolite that is responsible for its excellent retention of water [19]. In this regard, sepiolite is widely used as a bleaching agent, filter aid, industrial absorbent, and catalyst carrier [20]. As far as PLA/sepiolite nanocomposites are concerned, only a few studies have been reported in the literature. *Fukushima et al.* [21] reported the melt-elaboration and characterisation of PLA nanocomposites in the presence of sepiolite and montmorillonite. The addition of sepiolite into PLA matrix has shown to improve the fire-resistance of PLA matrix as well [22, 23].

The primary objectives of this work is to evaluate and to analyse the effect of different filler on the thermal, mechanical and fracture behaviour of PLA and the influence of secondary filler dimensionality, ~~namely sepiolite (1D) and talc (2D)~~, on thermomechanical performance of final ternary compounds. The effect of single loaded fillers (basalt, talc and sepiolite) and ternary systems (PLA/basalt/talc and PLA/basalt/sepiolite) were experimentally evaluated revealing significant enhancements of thermal, mechanical and degradation behavior of the neat PLA. The achieved performance could prompt engineering usage of the filled systems for specific applications with tailored performance, i.e. durability, 3D printing, increased thermal conductivity, high crystallinity percentage~~)~~.

2. Materials and Methods

2.1 Materials

The PLA matrix employed in this work is an Ingeo™ Biopolymer 3052D, purchased from NatureWorks, and characterized by a D-Lactide ~~with the~~ content of 1.4wt.%, a density of 1.24g/cm^3, with Tg of 55°C and a crystalline melt temperature of 145-160°C [24]. Silanized chopped basalt ~~fibre~~fibers type KV-12 were

purchased from Kammeny Vek with an initial length of 10 mm and a diameter of 10-22 μm. During injection molding significant fiber breakage of the millimeter sized basalt fibers occur; previous work [11] have measured the distribution of fiber length at different fiber content within the range from 5 to 40 wt%. By using direct analysis by optical microscopy of filled PLA/balsat manufactured samples, the average basalt fiber length was ranging from a maximum of 300 um (@5 wt%) to a minimum of 150 um (@ 40%) for the highest percentage.

Sepiolite was gently provided by Mi.Mac. (Capua, Italy). Fine particle sized talc type HTPUltra5 was purchased from Imifabi. All fillers were dried at 85°C for 6 hours to remove absorbed moisture during micronization and handling. PLA, basalt ~~fibre~~fibers, sepiolite and talc, were compounded with a LabTech LTE 26-44 twin screw extruder equipped with 26 mm diameter screws. The melting processing temperature was ~~at~~ 190°C, with a screw rotational speed of 20 min^{-1}.

The following system were manufactured and experimentally examined: A) neat PLA, B) single-filled PLA (PLA/basalt, PLA/sepiolite, PLA/talc) and also C) ternary systems (PLA/basalt/sepiolite and ~~the~~ PLA/basalt/talc) to investigate the influence of different dimensionality of the secondary fillers, respectively 1D-sepiolite and 2D-talc. Each of the PLA/basalt/talc and PLA/basalt/sepiolite ternary systems were manufactured using a two-stages process: 1) PLA and basalt fibers were mixed in the extruder, obtaining PLA/basalt pellets; 2) these pellets were extruded with the necessary amount of the ternary filler, either talc or sepiolite, and injection molded with the geometry required by the tests standards.

The employed basalt weight contents were 0, 10, 20 and 30 wt%, while the content of sepiolite and talc were 2, 5, 10 wt% and 5, 10, 15 wt%, respectively. A total of 28 samples ~~combinations~~ were produced and tested as listed in Table 1. Compounded materials were molded by using an Arburg Allrounder 370S 700-290 injection molding machine equipped with a 35 mm diameter screw employing a cooling time of 60 sec.

3. Testing methodology

3.1 Differential Scanning Calorimetry (DSC)

Thermal behaviour of neat PLA and PLA composite extruded granules was studied by Q-200 DSC supplied by TA Instruments, USA. Double scan tests were performed at the standard temperature rate of 10°C/min: the first scan (25-200°C) allows the system to erase previous memory so the second scan (25-200°C) would be independent by the thermal history undergone by the sample during the manufacturing process revealing the net effect of the filler presence. —Melting temperature (T_m), glass transition temperature (T_g), crystallization temperature (T_c) and melting enthalpy (ΔH_m) were determined by analysing the corresponding thermogram peaks according to thermal analysis procedure. The net effect of the filler on

composite crystallinity could be evaluated in two different ways: a) computing the ratio of enthalpy difference of the melting and cold crystallization over the fully crystallize PLA; b) evaluating the enthalpy of crystallization after the first scan during the cooling path. In this work, the degree of crystallinity was calculated from the corresponding values of melting enthalpy of the second scan according to the following relation:

$$X_c = \frac{\Delta H_m - \Delta H_{cold}}{\Delta H_{m100} * W_f} * 100 \qquad eq.1$$

where ΔH_m, ΔH_{cold}, and ΔH_{m100} are the enthalpies of melting, cold crystallization and 100% crystalline PLA taken as 93 J/g [22], respectively, while W_f is the weight percent of PLAs for the specific sample.

3.2 Thermogravimetric Analysis (TGA)

Thermal stability of manufactured neat ~~single~~, binay and ternary ~~filler~~ systems was studied by using a TGA Q500 branded TA Instruments under a nitrogen atmosphere (50 mL/min) and a heating ramp of 10°C/min. Sample weight of 5 ± 0.5 mg was considered for each run test from ambient temperature to 700°C.

3.3 Thermomechanical Analysis (TMA)

The thermomechanical behaviour of neat and filled PLA was investigated by a TMA 60 (Shimadzu, Japan) using a heating ramp of 5°C/min. The nominal dimensions of the TMA samples were 10X3X3 mm^3 according to ASTM E831-03. The Coefficients of Thermal Expansion (CTE), respectively, in the glassy phase (~~g~~CTE_g) and rubbery stage (~~r~~CTE_r), will be considered and analysed hereafter.

3.4 Thermal Conductivity Analysis

The thermal conductivity was measured by using a TCi Thermal Conductivity Analyzer (CTherm Technologies, Canada), which employs the Modified Transient Plane Source (MTPS) technique in characterizing the thermal conductivity and effusivity of material samples. The apparatus uses a one-sided, interfacial heat reflectance probe (diameter probe = 17mm) that applies a momentary constant heat source to the sample (with typical measurement pulse between 1 to 3 seconds). A minimum of five individual measurements was performed on bulk specimens (20X20X4 mm^3).

3.5 Mechanical Analysis (Tensile, Flexural, Dynamic Fracture)

Tensile and flexural (3-point bending) tests were performed on the injection moulded composites by using a Zwick Z020 universal testing machine (Zwick, USA) equipped with Zwick BZ 020/TN2S force

measuring cell with a force limit of 4kN. ASDM D638 and D790 standards were employed for tensile and flexural tests respectively, by using a cross-head speed of 5 mm/min.

Charpy tests were performed with a Coast Resil Impactor impact testing machine (CCSi Inc., USA) equipped with a 15 J impact energy hammer. For all mechanical tests, 6 specimens were tested, and ±2σ standard deviation was represented in the diagrams. Fractured surface analysis was performed by using a Jeol JSM 6380LA Scanning Electron Microscope (Jeol, Japan).

~~3.~~4. Results and Discussion

4.1 *Differential Scanning Calorimetry (DSC)*

Thermal behavior of neat and nanocomposite PLA samples were analyzed by DSC- considering both first and second scan on the same samples. Some interesting observations were drawn out to assess the effective contributions on the crystallinity degree of the final system, in the case of different fillers and their potential synergy.

Table 2 reports the computed values of crystallinity degree for all scanned samples according to the first DSC scan on micro-sized samples taken from extruded solid specimens. It is clear that variations of crystallinity due to the presence of the fillers were found negligible with an inconsistent trend. It is noteworthy to highlight that the level of crystallinity is almost null for the neat PLA system and this is expected considering the level of D-lactide very negligible (~4%).

The level of cristallinity, eventhough DSC data indicate a slightly variation of sample morphology from completely amourphose neat PLA to a semicristalline system (~3-6%), is changing neglegibly for all different filler contents and hybrid compositions. This reppresents a foundamental results to correctly understand and analyse the data obtained from thermo-mechanical characterization which will be later presented and discussed. In fact, variations measured in term of strength, modulus and strain will be ascribable to only fillers content and their specific morphology, without any effects referable to their actual crystallinity level.

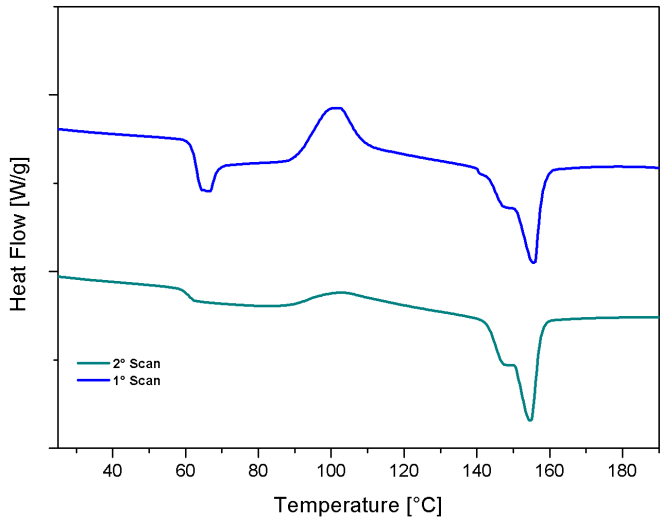

Figure 1.

The effect of the fillers and their synergy related to the morphology become more evident if the degree of crystallinity is computed on second DSC scan of the same sample. In fact, previous thermal history for all polymer systems represent a fundamental and critical issue for the forming amorphous/crystalline morphology and consequently for the physical-mechanical characteristics of the final applications. In order to comprehend in depth the influence of fillers and their synergy, it is mandatory to analyze in detail the thermal history that compounds undergo during injection ~~and~~ moulding processing stages. Neat and filled PLA compounds were processed by using injection ~~and~~ moulding, which imposes a very high cooling rate to the manufacturing sample material (i.e. mould temperature of 25°C with a material temperature of 170°C), and consequently a remarkably reduction of its crystallinity is foreseen. It is reasonable to assume that the effect of fillers is smoothed or muffled by the fast cooling rate associated to the processing conditions due to the limiting action in nucleation effect. Values of the degree of crystallinity, reported in Table 2, support this analysis; the filler content in any dimensional scale (microsized basalt fibers) and morphology (2D talc or 1D sepiolite) is not capable to trigger any additional as nucleation for new crystal sites and thus changes in crystallinity of the final PLA compounds are very restrained. Generally, for a semi-crystalline polymer, previous thermal history is erased completely when the temperature is above glass transition ($T>T_g$) or melting temperature ($T>T_m$) respectively for amorphous and crystalline polymer portions. In the case of semi-crystalline systems, the complete loss of previously frozen "memory" is achieved when the actual temperature of the system is above the melting point so both the amorphous and crystalline portions are completely "reset". In our case, at the end of the first DSC scan, as the temperature reach higher temperature that melting point (up to 200°C) all the previously stored "memory" is erased. When the polymers from above the glass transition temperature is cooled and then rescanned at the same

heating/cooling rate (standard heating ramp of 10°C/min), the fillers efficiently act as nucleating agents, leading to a significant increasing of the degree of crystallinity up to 24%, as in the case of 30B_15T samples (i.e. 30% micrometric basalt fibers and 15% nanometric 2D talc).

Fig. 1 shows the difference between first and second heating ramp performed on the PLA nanocomposites for the highest crystallinity variation, i.e. 30B_15T. Fig.2 shows the thermograms related to the second heating ramp performed on samples, while table 3 reports the corresponding results for all manufactured samples.

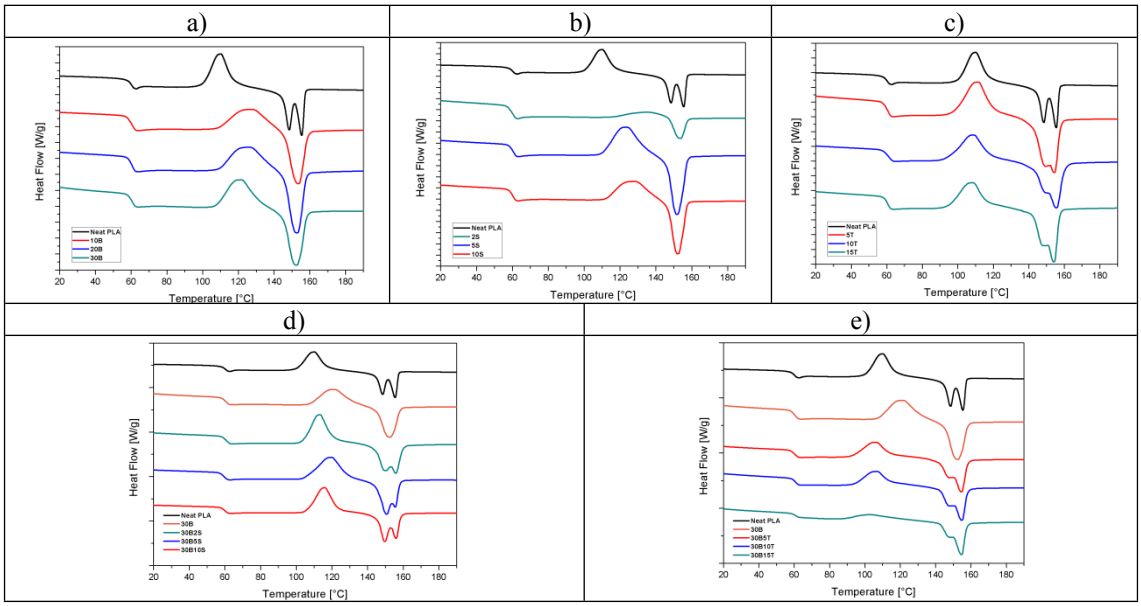

Figure 2.

According to Fig.2, it is clear that neat PLA is characterized by a bimodal melting peak at 145°C (T_{m1}) and 155°C (T_{m2}). This characteristic shaped peak is attributable to the formation of two different types of crystal structures, α and α' respectively, whose chain conformations (especially related to the side groups) is illustrated schematically in Fig. 3.

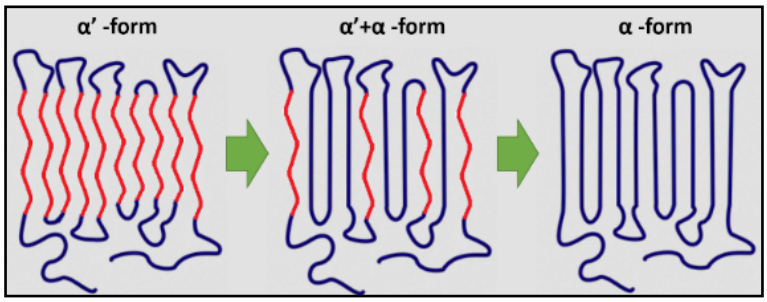

Figure 3.

The α-form (pseudo-orthorhombic, pseudo-hexagonal or orthorhombic [25]), melts at a higher temperature, while the α'-form (orthorhombic or trigonal [25]) melts in correspondence of the peak at a lower temperature. According to *Pan et al.* [26], the mechanism for the α-to-α' transformation, induced by high temperatures annealing, is a solid-solid transition process that involves the readjustment of the chain conformation and the packing of the macromolecular chains in a more energy-favourable state. It stands clearly (see thermograms in Fig. 2.c) that talc will prompt the persistence of a heterogeneous crystalline structure (α+α') characterized by the typical bimodal melting peak; whereas, the addition of 1D-shape fillers, i.e. sepiolite or basalt, will induced the formation of a single homogeneous crystalline phase characterized by a single melting temperature, as shown in Fig. 2.a and 2.b.

In the case of ternary system and in particular at higher basalt/sepiolite content (Fig 2.d), the heterogeneous α+α' crystalline structure becomes more stable than the homogeneous single structure observed in the binary PLA/basalt or PLA/sepiolite systems with the consequent splitting of the melting peak. Analogous behaviour is observed in Fig 1.e for the system PLA/basalt/talc.

The different effects of binary and ternary systems on crystalline structure (α and α' morphology) is reasonably related to the major filler surface energy which characterized the talc filler compared to the basalt or sepiolite, however this feature is persisting in the case of ternary compounds probably due to the major extent of filler network formed at higher concentration of basalt due to the particle contacts [26].

During re-heating (Fig. 2), neat and PLA binary and ternary compounds undergo a co-crystallization process above the glass transition experienced by the amorphous portion. The corresponding heat of transition, named as cold crystallization heat (ΔH_{cold}) at specific temperature (T_{cold}), indicates that the molecular chains of the amorphous portion have enough mobility to start ordering in a crystalline structure with lower energy barrier even at high temperature just before melting.

It is clear that the addition of the 2D talc nanoparticles is acting in the direction of narrowing the width of the co-crystallization peak, indicating the presence of a more relevant crystalline phase (higher crystallinity). This effect is much more pronounced for the PLA/basalt/talc ternary samples compared to other compositions. As reported in table 3, 30B_15T samples show a degree of crystallinity of X_m=24%, which corresponds to an increase of 650% if compared to the measured crystallinity for neat PLA sample. This data proof that 2D nanometric talc effectively will act as an efficient nucleating agent particularly in synergy with micrometric basalt ~~fibre~~fibers. On the other hand, Table 3 highlights that sepiolite and basalt do not activate any relevant nucleating action to increase crystallinity degree if compared to the neat hosting matrix. From the DSC data, also the glass transition temperatures of the binary and ternary compounds

were measured and analyzed. As reported in table 3, a negligible effect on glass transition temperature is performed by the presence of the different fillers, as the value of Tg for the neat PLA is almost unchanged for all percentage and typology of filler loadings (T_g^{PLA} ~60°C). [3]

4.2 *Thermogravimetric Analysis (TGA)*

Thermal degradation of neat PLA and PLA nanocomposites was analyzed by using Thermal Gravimetrical Analysis (TGA) and results are listed in table 3, where $T^{5\%}$ and $T^{50\%}$ are the temperatures associated to 5% and 50% weight loss respectively. Fig. 4 shows TGA curves, in an inert atmosphere, for the PLA binary nanocomposites, i.e. PLA~~+~~/basalt (Fig. 4.a), PLA/~~+~~sepiolite (Fig. 4.b) and PLA~~+~~/talc (Fig. 4.c). All systems exhibit thermal degradation and significant weight loss with temperature, following a single characteristic step mechanism of degradation.

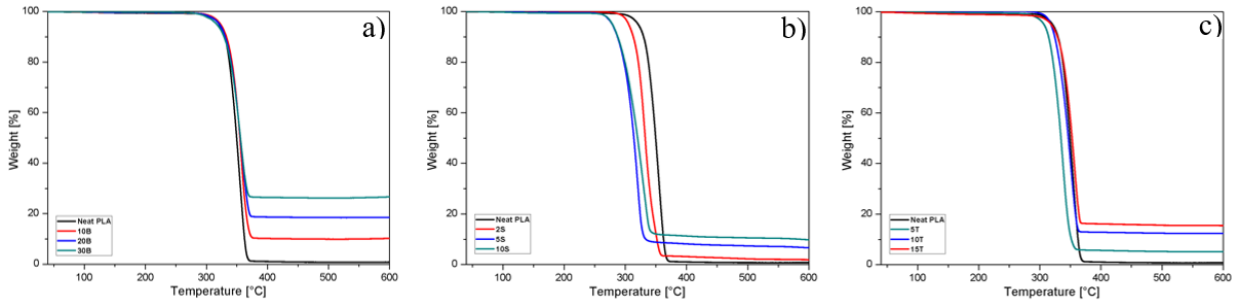

Figure 4.

From fig. 4.a, it is clear that basalt ~~fibre~~fibers do not influence remarkably the thermal stability (changing of $T^{50\%}$) of the hosting matrix. As reported in [27], sepiolite is known to catalyse the degradation reactions of the polymeric matrix, reducing the thermal stability of the resulting nanocomposite. This is observable also in fig. 4.b for a low sepiolite contents. Anyway, increasing the filler content, it is observable a trend inversion (a slight increase of thermal stability for 5S and 10S specimens). This effect could be associated to the inorganic nature of sepiolite and also to its capacity of acting as barrier for volatiles produced during decomposition process leading to a progressive delaying of sample weight loss, as also supported by *Sabzi et al.* [28]. For the samples filled with talc, an analogous trend is appreciable; i.e. a thermal stability reduction for low weight contents followed by an increase of thermal stability for higher weight contents. It is noteworthy to note that the lower specific surface of talc (2D filler), compared to sepiolite (1D filler), will limit its catalytic effect on the PLA degradation reactions therefore, at low weight content, the detrimental effect on thermal stability will results smaller if compared to the analogous action of the sepiolite filler. For all samples, the increased weight residue is surely due to the presence of fillers loading the hosting system, whose degradation is prevented by their inorganic nature at the relatively low scanning temperature.

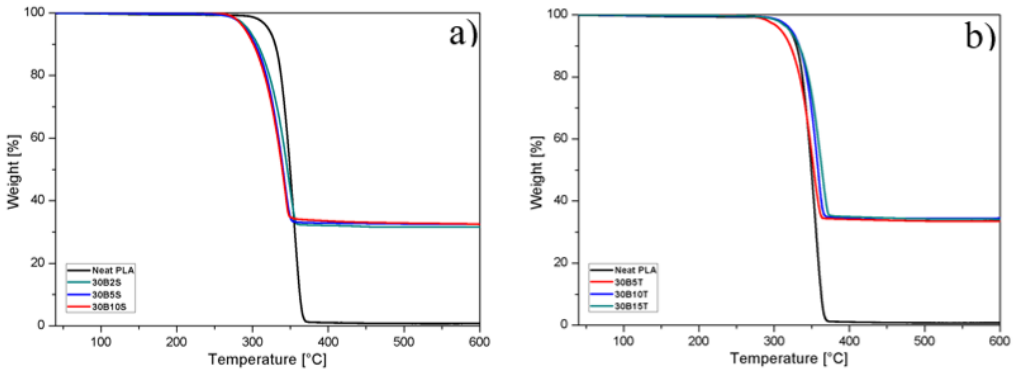

Figure 5.

For what the hybrid systems PLA/basalt/sepiolite and PLA/basalt/talc is concerned (refer to fig. 5 and table 2), it is observable a very slight reduction of thermal stability in both cases if compared to the neat PLA. In particular, for PLA/basalt/sepiolite, the higher the basalt content the lower is the thermal stability mainly due to the sepiolite presence ($T^{50\%}_{10B\_2S}$ = 354°C, $T^{50\%}_{10B\_10S}$ = 323°C: $\Delta T^{50\%}_{10B\_S}$ = 31°C; $T^{50\%}_{30B\_2S}$ = 346°C, $T^{50\%}_{30B\_10S}$ = 339°C: $\Delta T^{50\%}_{30B\_S}$ = 7°C), indicating that basalt percentage will limit the sepiolite thermal stability reduction.

4.3 *Thermomechanic Analysis (TMA)*

The dimensional stability is a critical factor for composites in different applications. Poor dimensional stability determines unwanted changes in shape during processing and life service for components and structures limiting also material performance, i.e. thermal shock resistance or bulk integrity. The coefficient of thermal expansion (CTE) is a dimensional stability parameter, generally high for polymers compared to metals and ceramics. Polymer high CTE values are attributable to the presence of free volume in macromolecular structures which can induces freely movements of the chains with temperature level. The addition of an inorganic filler can reduce the available free volume level limiting chains mobility with a remarkable reduction of the CTE. The linear coefficient of thermal expansions wasere measured below (CTE_g) and above (CTE_r) the glass transition temperature of the compounds and results are listed in Table 4. According to the literature [29], the incorporation of inorganic fillers in the PLA matrix decreased the CTE values, especially at high filler contents. As shown in table 4, highest basalt content reduces the CTEg and CTE_r values of about 29.5% and 36.4%, respectively. The highest CTEg and CTE_r reductions are associated to the samples 30B_5S (ΔCTE_g=36.1% and ΔCTE_r=41.2%) and 30B_10T (ΔCTE_g=53.9% and ΔCTE_r=45.3%).

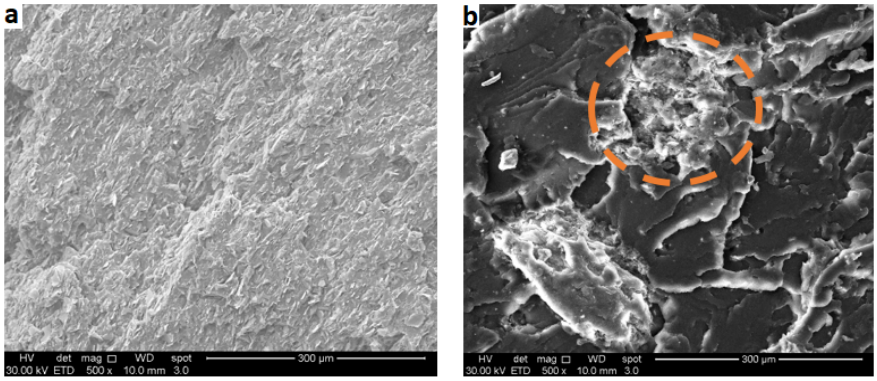

Figure 6.

The further increase of filler does not reduces correspondingly the compounds thermal coefficient value likely due to the decrease of homogeneity associated to the formation of large filler inconsistent agglomerations. From data of table 4 it is clear that, at same filler contents, talc induces a greater reduction of CTEs values compared to sepiolite: this effect could be attributable to the better dispersion of talc in the PLA matrix compared to sepiolite. As shown in the micrograph of fig. 6.b, sepiolite leads to the formation of large and incoherent aggregates, likely due to its strong tendency to aggregation [28]. Whereas, as shown in fig. 6.a, talc nanoplatelets are dispersed more efficiently with an highly exfoliated structure. The major interface boundary among the 2D talc nanoparticles and hosting matrix will restrain matrix thermal expansion reducing CTE of both glassy and rubbery state of the final compound.

4.4 Thermal Conductivity Analysis

As reported by *Strumpler et al.* [30], fillers with high aspect ratio, such as fibers (sepiolite) and platelets (talc), can form more continuous thermally conductive pathways in the polymer matrix and thus are more effective in enhancing the thermal transfer. Moreover, also the size of the employed fillers plays a key role in the enhancement of nanocomposites thermal conductivity, since it was demonstrated that composites with finer fillers are characterized by higher thermal conductivities [31, 32].

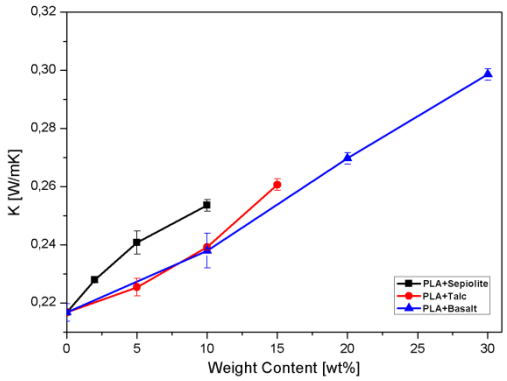

Figure 7.

Fig. 7 shows thermal conductivity (*K*) results for the PLA/basalt, PLA/talc and PLA/sepiolite binary systems. Analyzing the reported data, the following observations could be drawn out:

a. being constant the filler content, it is evident that sepiolite induces an higher enhancement of the thermal conductivity compared to talc, and this effect is reasonable associated to the shape and aspect ratio of sepiolite fibrillary structure (1D shape – see Fig. 8). Spindly morphology of the sepiolite is particularly effective in providing good particle-to-particle contact leading to a more efficient transfer heat mechanism by forming a continous path with a good interface mong nanoparticles. 2D shaped talc nanoplatelets due to gemetrical constrains do not lead to analogous clustering morphology thus reporting a limited efficiency in network formation and this explains the lower thermal conductivity enhancement of this filler based nanocomposites compared to corresponding weight content of sepiolite based nanocomposites;

b. at the same filler contents, the remarkable difference in terms of thermal conductivity between sepiolite and basalt based compounds could be referred to difference in particles relative dimensions; in fact, although basalt and sepiolite have the same shape (i.e. fiber-like geometry), the nanometric geometry of the sepiolite ~~will~~ will prompt a high concentration of particle contacts compared to the basalt forming a more 3Dmensional continous path for heat transfer if compared to morphology of basalt based compounds;

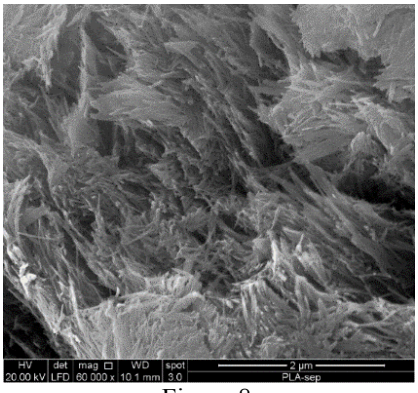

Figure 8.

Table 5 and Fig. 9 resume the thermal conductivity results of both ternary systems, respectively PLA/basalt/talc and PLA/basalt/sepiolite at considered percentage; samples 30B_10S and 30B_15T are characterized by the highest improvement in term of thermal conductivity, i.e. 57% and 79% respectively.

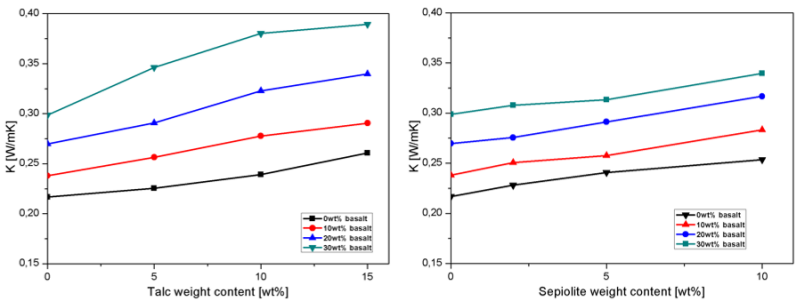

Figure 9.

It is noteworthy that in the hybrid systems PLA/basalt/sepiolite, basalt content act as a limiting agent for the sepiolite regarding thermal conductivity performance, as an increase of basalt content reduces the specific (i.e. per unit percentage of sepiolite) effect of the nanofiller (see the slope of k vs. basalt content in fig. 10). On the other hand, basalt microfibers tend to enhance the efficiency of talc as thermal conductivity filler, as increasing in basalt percentage improve the derivative of the thermal conductivity with respect the basalt content (fig. 10). This behavior could be attributable to an improving effect of the synergy for due to the difference in shape between talc (2D filler) and basalt (1D filler). Morphology of the final system tends to be more compact and consistent for the basalt/talc filler compared to basalt/sepiolite; the reduced average distance and the high probability of contact location in the case of 2D nanosized talc and micrometric 1D basalt fiber enhance efficiently the heat transfer mechanism determining a high thermal conductivity performance of the final compounds. The analysis of thermal conductivity data has revealed that sepiolite induced a significant increase compared to the talc and basalt fibers likely due to the higher aspect ratio (being constant the weight content). It is noteworthy that, while basalt limits the efficiency of sepiolite as thermal conductivity filler, hybrid systems made of talc and basalt are characterized by the highest thermal conductivity values caused by a synergic effect between talc and basalt (likely associated to their different geometry). The variations compared to the neat PLA are associated with the samples 30B_10S and 30B_15T a, i.e. 57% and 79% respectively.

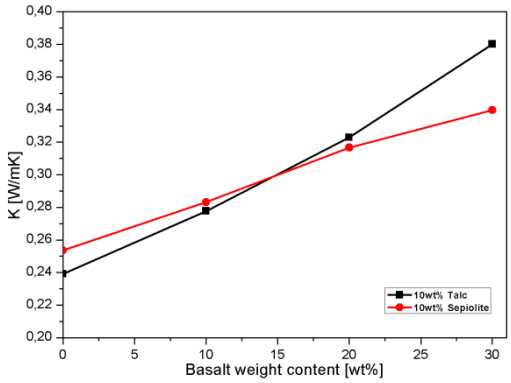

Figure 10.

4.5 *Mechanical Analysis*

Injection moulded samples were mechanical characterized by means of tensile, bending and impact (Charpy) tests. Obtained results determine that all fillers linearly increase the elastic modulus of the PLA matrix (fig. 11), and this effect is associated to the higher moduli of the fillers compared to the hosting matrix (85 GPa [33], 170 GPa [34] and 10.6 GPa [35] for basalt, talc and sepiolite, respectively). Despite the higher elastic modulus of talc platelet compared to basalt fibers, the shape and the orientation of the basalt fibers induce an higher stiffening effect in the PLA matrix, with a maximum increase of elastic

modulus of about 121%. Fig. 11 reports the tensile strength for the PLA/basalt, PLA/talc and PLA/sepiolite systems, and three different behaviors are observable:

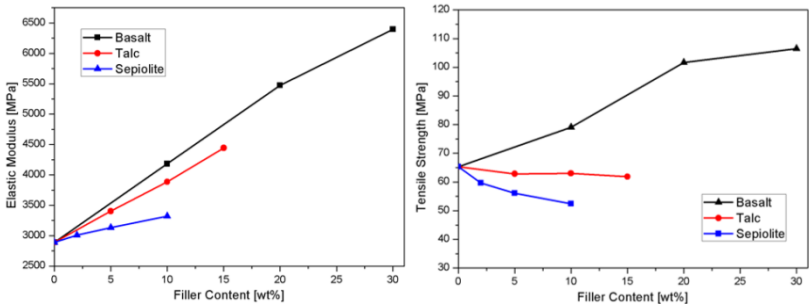

Figure 11.

1) basalt fibers induce a linear increase of the tensile strength up to 106 MPa for the 30wt% loaded sample, and this remarkable increase is attributable to the excellent adhesion found between the PLA and the basalt fibers (Fig. 12); the improved adhesion at interface between basalt fiber and PLA matrix due to the pre-silanization treatment of the inorganic filler, lead to an efficient stress transfer mechanism which increases final tensile strength;

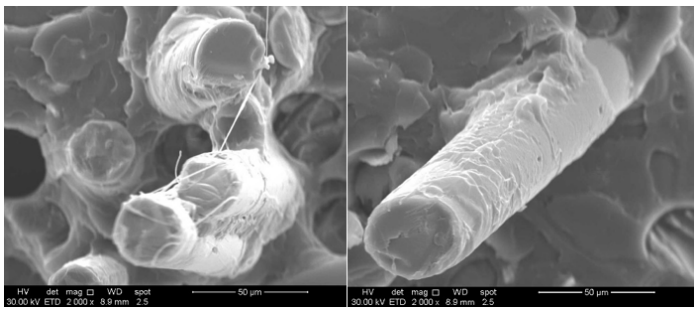

Figure 12.

2) talc platelets induce slight reduction of the tensile strength, in agreement with literature; in fact, according to Fowlks et al. [36], particulate fillers (talc) tend to decrease the strength of the composites due to their lower ability to support stresses transferred from the polymer matrix;
3) although sepiolite is characterized by higher aspect ratio respect to talc filler (larger aspect ratio leads to higher reinforcement [37]), the sepiolite based compounds exhibit significantly lower strength compared to the PLA/talc at the same filler content; this effect is associated to the formation of large sepiolite clusters with incoherent structure, as shown in fig. 6;

When talc was also added to the basalt reinforced composites, elastic modulus increases remarkably (fig. 13), with a maximum variation of ~170% for the sample 30B_15T. Sepiolite fibers, instead, lead to a detrimental final effect: at lower basalt content (10wt%), the addition of sepiolite do not induce anychange in elastic modulus (i.e. 0.45% in the sample 10B_10S) compared to the sample 10B; conversely, for the system characterised by higher basalt contents the presence of sepiolite leads even to a reduction of the elastic modulus (up to 11% for sample 30B_10S) compared to the corresponding 30B samples with just

basalt loading. Therefore, in the PLA/basalt/sepiolite, storage modulus is generally higher than neat PLA but this positive effect is ~~inherently~~ linked inherently with the only presence of basal fiber and not any hoe associate to the secondary filler.

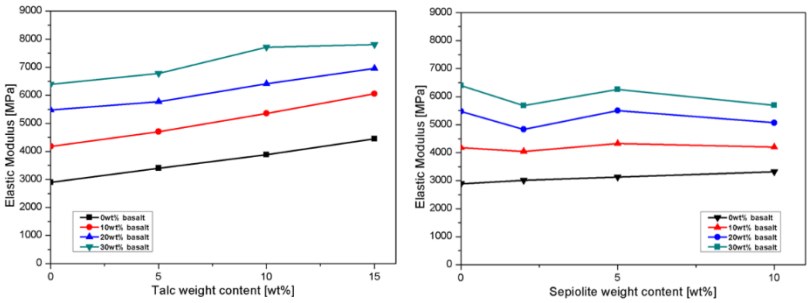

Figure 13.

For what the tensile strength is concerned (Fig. 14), talc and sepiolite does not induce a positive effect to the basalt filled compounds: in fact, the maximum increase of tensile strength, i.e. 63%, is associated to the sample filled with 30wt% of basalt (30B), while the addition of the highest content of talc (15wt%) and sepiolite (10wt%) lead to a lower increase of the tensile strength, i.e. 46% and 6% respectively.

Similar trends are found for bending properties (Figs. 15-17). The maximum variation of bending modulus (+261%) is related to the hybrid system 30B_15T, while the system 30B_10S is characterized by a storage modulus of about 7379 MPa, lower compared to the corresponding 30B PLA/basalt binary system, which reveal a substantial increasing of the modulus of about 167%.

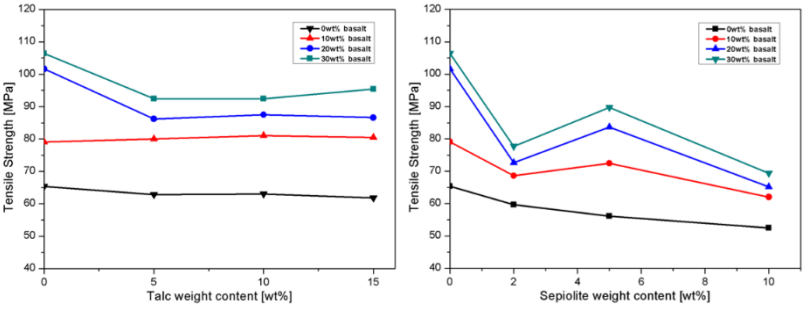

Figure 14.

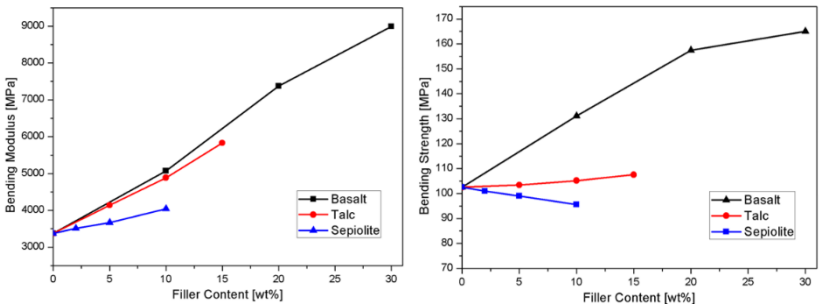

Figure 15.

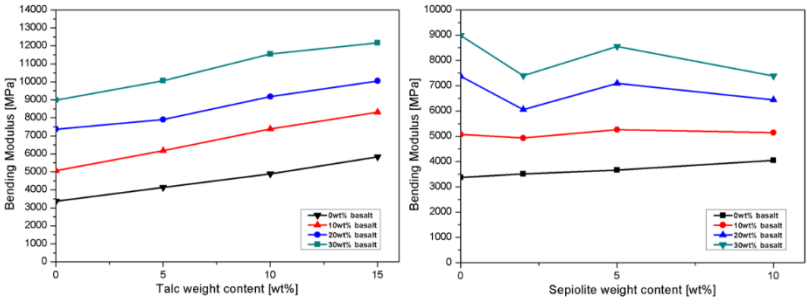

Figure 16.

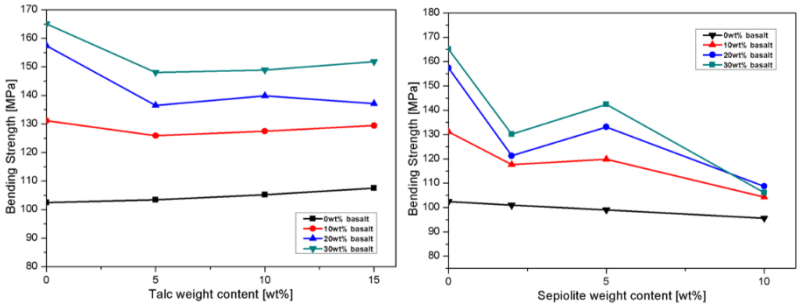

Figure 17.

The addition of talc or sepiolite to the basalt filled composites reduces the bending strength compared to the equivalent basalt filled samples; in fact, samples 30B, 30B_15T and 30B_10S are characterized by a bending strength of 165 MPa, 151 MPa and 106 MPa respectively, which correspond to an increase of about 62%, 48% and 4% compared to the neat PLA.

-PLA is classified as brittle material [38], and for this reason the impact strength of the injection moulded compounds should be measured and analyzed. It results clear in Fig. 18 that binary systems, PLA/basalt and PLA/talc, show a high impact strength compared to the hybrid ternary system, PLA/basalt/talc; in fact, the addition of 20 wt% of basalt fibers or 5 wt% of talc platelets increases the impact strength up to 43.8 kJ/m^2 and 59.2 kJ/m^2 respectively, with an overal improvement of ~97% and ~140% compared to the neat PLA (24.7 kJ/m^2). Whereas, in the hybrid ternary system reveals a limited increase of the impact strength of only ~31%, as in the case of 20B_5T sample (i.e. 32.3 kJ/m^2) compared to the neat PLA. According to the obtained mechanical and impact tests, it stands clear that the addition of sepiolite induces always a detrimental effect over the performance of the final compounds.

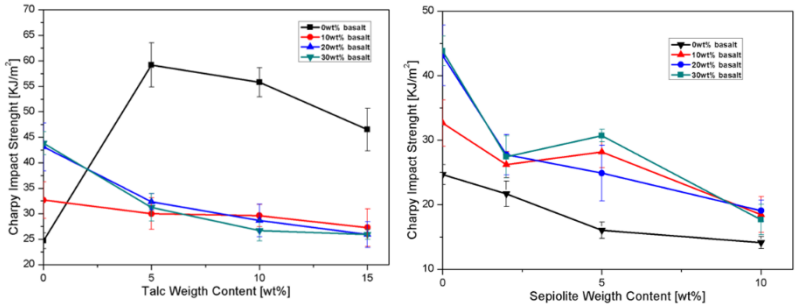

Figure 18.

5. Conclusions

This work reports the effect of the talc and sepiolite on thermal and mechanical properties of PLA/basalt composites. In particular, we have studied the effects a 2D talc nanoplatelets and 1D sepiolite nanofibers. Filler concentrations from 10-30wt% for basalt, 5-15wt% for talc and 5-10wt% for sepiolite have been employed. The basalt ~~fibre~~fibers~~ ~~fibers increased the thermal stability of the hosting matrix, acting as a barrier for the heat transfering. Conversely, low content of basalt and talc resulted in a slight reduction in thermal stability caused by possible degradation from photocatalytical effects to the PLA matrix. Thermomechanical analysis has revealed that the talc reduced remarkably the matrix CTEs (both above and below a glass transition temperature) and this effect could be attributed to the best dispersion of talc nanoplatelets in the PLA matrix compared to that achieved with sepiolite ~~fibre~~fibers. The maximum reduction of CTE was associated with the sample 30B_10T, i.e. 53.9% and 45.3% for CTE below and above T_g, respectively.

Tensile and flexural results showed that talc and basalt addtives efficiently enhanced the moduli of the composites for the hybrid system 30B_15T (170% and 261% respectively). Regarding the tensile and bending strength, the highest values are of the binary system 30B (63% and 62%, respectively). In these cases, the additional talc or sepiolite in compositions drastically reduced their strength.

The impact properties were remarkably increased with addition of talc and basalt at low range of weight contents. Whereas for the hybrid systems~~–~~, PLA/basalt/talc, a significant detrimental cross-effect was observed which ~~drastically~~ reduces drastically impact property compared to the performance shown by the single binary systems (impact energy 43.8 kJ/m^2 for 20B, 59.2 kJ/m^2 for 5T and 32.3 kJ/m^2 for the sample 20B_5T). Among the three different fillers, sepiolite ~~revealed~~ showed the more ~~a relevant~~ detrimental effect on mechanical performance likely due to the achieved poor dispersion inherently related to the nanofiller tendency to agglomerate as inconsistent clustered structured at micro-level.

Acknowledgement

This publication was supported by the Italian–Hungarian agreement of the Hungarian Academy of Sciences. We would like to thank Mr. Fabio Docimo for his support in sample manufacturing and Ms. Mariarosaria Marcedula and Ms. Alessandra Aldi for the thermal analysis test performed at IPCB Lab. ~~-~~All data will be available to the readers upon request.

References

[1] Chandra R, Rustgi R. Biodegradable polymers. Prog. Polym. Sci. 1998; 23:1272-1335.

[2] Lim LT, Auras R, Rubino M. Processing technologies for poly(lactic acid). Prog. Polym. Sci. 2008; 33:820-852.

[3] Li H, Huneault MA. Effect of nucleation and plasticization on the crystallization of poly(lactic acid). Polym. 2007; 48:6855–6866.

[4] Kolstad JJ. Crystallization kinetics of poly(L-lactide-co-mesolactide). J. Appl. Polym. Sci. 1996; 62:1079–1091.

[5] Mathew AP, Oksman K, Sain M. The Effect of Morphology and Chemical Characteristics of Cellulose Reinforcements on the Crystallinity of Polylactic Acid. J. Appl. Polym. Sci. 2006; 101:300–310.

[6] Espino-Pe´rez E, Bras J, Ducruet V, Guinault A, Dufresne A, Domenek S. Influence of chemical surface modification of cellulose nanowhiskers on thermal, mechanical, and barrier properties of poly(lactide) based bionanocomposites. Eur. Polym. J. 2013; 49:3144–3154.

[7] Harris AM, Lee EC. Improving mechanical performance of injection molded PLA by controlling crystallinity. J. Appl. Polym. Sci. 2008; 107:2246–2255.

[8] Fortunati E, Armentano I, Zhou Q, Puglia D, Terenzi A, Berglund LA, Kenny JM. Microstructure and nonisothermal cold crystallization of PLA composites based on silver nanoparticles and nanocrystalline cellulose. Polym. Degrad. Stabil. 2012; 97:2027–2036.

[9] Han H, Wang X, Wu D. Preparation, crystallization behaviors, and mechanical properties of biodegradable composites based on poly(L-lactic acid) and recycled carbon fiber. Compos. Part A-Appl. S. 2012; 43:1947–1958.

[10] Fiore V, Scalici T, Di Bella G, Valenza A. A review on basalt fiber and its composites. Compos. Part B-Eng. 2015; 74:74-94.

[11] Tábi T., Zoltán A. É., Tamás P., Czigány T., Kovács JG Investigation of injection moulded poly(lactic acid) reinforced with long basalt fibres Composite Part A 2014, 64:99-106.

[12] Czigány T, Kovács JG, Tábi T. Basalt fiber reinforced poly(lactic acid) composites for engineering applications. In: Proceedings of ICCM19 Conference. Montreal, July, 2013. p. 4377-4384.

[13] Battegazzore D, Bocchini S, Frache A. Crystallisation kinetics of poly(lactic acid)-talc composites. Express Polym. Lett. 2011, 5:849-858.

[14] Harris AM, Lee EC. Improving mechanical performance of injection molded PLA by controlling crystallinity. J. Appl. Polym. Sci. 2008; 107:2246-2255.

[15] Jain S, Misra M, Mohanty AK. Thermal, mechanical and rheological behavior of Poly(lactic acid)/Talc Composites. J. Polym. Environ. 2012; 20:1027-1037.

[16] Russo P, Acierno D, Vignali A, Lavorgna M. Poly(lactic acid)-based Systems filled with talc microparticles: thermal, structural and morphological issues. Polym. comp. 2014; 35(6):1093-1103.

[17] Huda MS, Drzal LT, Mohanty AK, Misra M. The effect of silane treated- and untreated-talc on the mechanical and physico-mechanical properties of poly(lactic acid)/newspaper fibers/talc hybrid composites. Compos. Part B-Eng 2007; 38:367-379.

[18] Sekelik DJ, Stepanov EV, Nazarenko S, Schiraldi D, Hiltner A, Baer E. Oxygen barrier properties of crystallized and talc-filled poly(ethylene terephthalate). J. Polym. Sci. Part B: Polym. Phys. 1999; 37:847.

[19] Zotti A, Borriello A, Martone A, Antonucci V, Giordano M, Zarrelli M. Effect of sepiolite filler on mechanical behaviour of a bisphenol A-based epoxy system. Compos. Part B-Eng. 2014; 67:400-409.

[20] Alvarez A. Sepiolite: Properties and Uses. Dev Sedimentol 1984; 37:253-287.

[21] Fukushima K, Tabuani G, Camino G. Nanocomposites of PLA and PCL based on montmorillonite and sepiolite. Mater. Sci. Eng. C 2009; 29(4):1433-1441.

[22] González A, Dasaria A, Herrero B, Plancher E. Fire retardancy behavior of PLA based nanocomposites. Polym. Degrad. Stabil. 2012; 97(3):248-256.

[23] Zotti A, Borriello A, Ricciardi M, Antonucci V, Giordano M, Zarrelli M. Effects of sepiolite clay on degradation and fire behaviour of a bisphenol A-based epoxy. Compos. Part B-Eng. 2015; 73:139-148.

[24] Technical Data Sheet Ingeo™ Biopolymer 3052D. NatureWorks, Minnetonka; 2002.

[25] Yasuniwa M, Tsubakihara S, Iura K, Ono Y, Dan Y, Takahashi K. Crystallization behavior of poly(l-lactic acid). Polym. 2006; 47:7554-7563.

[26] Pan PJ, Zhu B, Kai WH, Dong T, Inoue Y. Polymorphic Transition in Disordered Poly(L-lactide) Crystals Induced by Annealing at Elevated Temperatures. Macromol. 2008; 41:4296-4304.

[27] Chen H, Zheng M, Sunand H, Jia Q. Characterization and properties of sepiolite/polyurethane nanocomposites. Mater. Sci. Eng. A 2007; 445:725-730.

[28] Sabzi M, Jiang L, Atai M, Ghasemi I. PLA/Sepiolite and PLA/Calcium Carbonate Nanocomposites: A Comparison Study. J. Appl. Polym. Sci. 2013; 129:1734–1744.

[29] Lee H, Fasulo PD, Rodgers WR, Paul DR. TPO based nanocomposites. Part 2. Thermal expansion behavior. Polym. 2006; 47:3528–3539.

[30] Strumpler R, Glatz-Reichenbach J. Conducting Polymer Composites. J. Electrochem. Soc. 1999; 3,4:329-346.

[31] Zhou WY, Wang CF, Ai T, Wu K, Zhao FJ, Gu Z. A novel fiber-reinforced polyethylene composite with added silicon nitride particles for enhanced thermal conductivity. Compos. Part A-Appl. S. 2009; 40:830–836.

[32] Kemaloglu S, Ozkoc G, Aytac A. Thermally conductive boron nitride/SEBS/EVA ternary composites: Processing and characterization. Polym. Compos. 2010; 31:1398–1408.

[33] Soares B, Preto R, Sousaa L. Mechanical behavior of basalt fibers in a basalt-UP composite. Procedia Structural Integrity 2016; 1:82–89.

[34] Martinatti F, Ricco T. High-rate fracture toughness of polypropylene-based, hybrid, particulate composites. J. Mater. Sci. 1994; 29:442-448.

[35] Frydrych M, Wan C, Stengler R. Structure and mechanical properties of gelatin/sepiolite nanocomposite foams. J. Mater. Chem. 2011; 21:9103-9111.

[36] Fowlks AC, Narayan R. The Effect of Maleated Polylactic Acid (PLA) as an Interfacial Modifier in PLA-Talc Composites. J. App. Pol. Sci. 2010; 118:2810–2820.

[37] Martone A, Faiella G, Antonucci V, Giordano M, Zarrelli M. The effect of the aspect ratio of carbon nanotubes on their effective reinforcement modulus in an epoxy matrix. Compos. Sci. Technol. 2011; 71(8):1117-1123.

[38] Zotti A, Borriello A, Zuppolini S, Antonucci V, Giordano M, Pomogailo AD, Lesnichaya VA, Golubeva ND, Bychkov AN, Dzhardimalieva GI, Zarrelli M. Fabrication and characterization of metal-core carbon-shell nanoparticles filling an aeronautical composite matrix. Eur. Polym. J. 2015; 71:140-151.

Figure Captions

Figure 1 - Comparison between DSC first and second heating ramp for the sample 30B_15T.

Figure 2 - DSC thermogram of neat PLA and PLA nanocomposites (2th heating cycle): a) PLA+Basalt, b) PLA+Sepiolite, c) PLA+talc, d) PLA+Basalt(30wt%)+Sepiolite and e) PLA+Basalt(30wt%)+talc.

Figure 3 - Schematic illustration of PLA α-to-α' transformation after annealing [24].

Figure 4 - TGA scans of a) PLA/basalt, b) PLA/sepiolite and c) PLA/talc systems.

Figure 5 - Effect of 30 wt% basalt with a) sepiolite and b) talc on thermal stability of final compounds.

Figure 6 - SEM images of a) PLA/talc and b) PLA/sepiolite systems (circled picture identifies sepiolite agglomerates).

Figure 7 - Thermal conductivity of PLA/basalt, PLA/talc and PLA/sepiolite systems.

Figure 8 - SEM micrograph of agglomerated fibrillary sepiolite formation.

Figure 9 - Thermal conductivity of PLA/basalt/talc and PLA/basalt/sepiolite systems.

Figure 10 - Comparison between thermal conductivity vs. basalt content at fixed talc or sepiolite concentration (10wt%).

Figure 11 - Elastic modulus (left) and tensile strength (right) of PLA+basalt, PLA+talc and PLA+sepiolite systems.

Figure 12 - Fractured surface images of basalt reinforced PLA composites.

Figure 13 - Elastic modulus of PLA+basalt+talc (left) and PLA+basalt+sepiolite (right) systems.

Figure 14 - Tensile strength of PLA+basalt+talc (left) and PLA+basalt+sepiolite (right) systems.

Figure 15 - Bending modulus (*left*) and tensile strength (*right*) of PLA/basalt, PLA/talc and PLA/sepiolite systems.

Figure 16 - Bending modulus of PLA/basalt/talc (left) and PLA/basalt/sepiolite (right) systems.

Figure 17 - Bending strength of PLA/basalt/talc (left) and PLA/basalt/sepiolite (right) systems.

Figure 18 - Unnotched Charpy impact strength of PLA/basalt/talc (left) and PLA/basalt/sepiolite (right).

Tables

Filler content	**Basalt wt%**			
	0	**10**	**20**	**30**
0	PLA	10B	20B	30B
Sepiolite wt%				
2	2S	10B_2S	20B_2S	30B_2S
5	5S	10B_5S	20B_5S	30B_5S
10	10S	10B_10S	20B_10S	30B_10S
Talc wt%				
5	5T	10B_5T	20B_5T	30B_5T
10	10T	10B_10T	20B_10T	30B_10T
15	15T	10B_15T	20B_15T	30B_15T

Table 1 - Abbreviation of the produced composites.

Filler content	**Basalt wt%**			
	0	**10**	**20**	**30**
	0	4	1.7	5.6
Sepiolite				
2	3	1.3	8.7	5.5
5	4.9	4.1	4.1	3.4
10	4.8	1.7	2.7	4.1
Talc				
5	1.8	6.6	8	4.9
10	3.1	2.5	6.4	2.7
15	4.1	6.3	5.5	1.6

Table 2 - Neat PLA and PLA compounds grade of crystallinity obtained by the DSC first heating ramp.

Samples	**T_g [°C]**	**T_{m1} [°C]**	**T_{m2} [°C]**	**T_{cold} [°C]**	**ΔH_{cold} [J/g]**	**ΔH_m [J/g]**	**X_m [%]**	**$T^{5\%}$ [°C]**	**$T^{50\%}$ [°C]**	**Residual [%]**
PLA	60	145	155	110	28.5	31.5	3.2	320	349	0.8
10B	60	154	154	127	16.2	17.8	1.9	323	355	9.9
20B	60	153	153	126	17.7	20.8	4.1	321	356	18.4
30B	60	152	152	121	18.6	19.2	0.9	317	356	26.7
2S	60	154	154	135	5.9	7.8	2.1	305	332	2.1
5S	61	152	152	123	25.0	25.9	1.1	278	314	6.9
10S	60	152	152	127	19.0	20.8	2.2	278	320	10.2
10B_2S	60	152	152	124	22.4	24.2	2.1	315	354	10.3
10B_5S	61	153	153	125	19.5	22.3	3.5	295	342	15.6
10B_10S	61	154	154	128	16.7	17.9	1.6	277	323	20.1

20B_2S	60	149	155	115	21.8	23.7	2.7	295	347	22.9
20B_5S	60	153	153	130	13.7	16.6	4.2	290	338	23.5
20B_10S	60	150	155	118	22.3	23.1	1.2	280	333	27.9
30B_2S	60	150	156	113	22.7	24.9	3.4	293	346	31.5
30B_5S	60	151	156	119	21.6	24.5	4.8	290	340	32.5
30B_10S	60	150	156	116	19.4	19.6	0.4	287	339	31.8
5T	60	149	154	111	23.7	25.3	1.9	306	334	5.2
10T	61	149	155	109	18.1	22.6	5.4	318	347	12.4
15T	60	148	154	108	19.1	23.0	4.9	318	353	15.6
10B_5T	57	153	153	124	22.6	25.8	4.1	332	358	14.7
10B_10T	61	148	154	108	17.2	24.0	9.1	325	358	16.7
10B_15T	60	147	154	104	12.4	21.9	13.4	322	360	29.4
20B_5T	61	148	154	109	18.9	23.7	6.8	321	362	26.8
20B_10T	60	147	154	106	12.3	21.5	14.1	318	357	28.6
20B_15T	61	148	154	105	10.2	20.3	16.7	320	361	33.1
30B_5T	60	148	155	106	13.4	19.4	9.7	309	356	33.5
30B_10T	61	148	155	107	12.4	19.3	12.2	323	358	34.1
30B_15T	61	148	155	103	5.7	18.0	24.0	321	363	34.9

Table 3 - DSC (second scan) and TGA results of neat PLA and PLA nanocomposites.

	CTE < Tg = CTEg x 10^6 [K^{-1}]				**CTE > Tg = CTEr x 10^6 [K^{-1}]**			
	basalt wt%				**Basalt wt%**			
	0	10	20	30	0	10	20	30
0	96.9	88.2	73.8	68.3	193.9	162.3	125.0	123.4
Sepiolite								
2	88.0	77.6	69.1	62.4	184.2	160.1	151.6	131.4
5	84.9	76.2	67.3	61.9	171.4	159.1	146.3	114.0
10	78.9	72.9	64.5	68.5	169.2	154.3	141.2	115.8
Talc								
5	86.4	66.9	55.2	56.3	179.0	151.6	130.0	126.5
10	75.9	60.1	50.2	44.6	164.8	133.4	124.5	106
15	63.1	59.8	48.5	49.4	141.9	130.3	107.2	108.1

Table 4 - TMA results of neat PLA and PLA nanocomposites.

	K – Thermal Conductivity **[W/mK]**			
	basalt wt%			
	0	**10**	**20**	**30**
0	0.217	0.238	0.270	0.299
sepiolite				
2	0.228	0.251	0.276	0.308
5	0.241	0.258	0.291	0.313
10	0.254	0.283	0.317	0.340
talc				
5	0.225	0.256	0.291	0.346
10	0.239	0.278	0.323	0.380
15	0.261	0.291	0.340	0.389

Table 5 - Thermal conductivity results of neat PLA and PLA nanocomposites.